1556
doi:10.1017/S1431927619008511
Microsc. Microanal. 25 (Suppl 2), 2019

Cavities Imaged by In-Line Electron Holography in Irradiated Aluminium Alloy

Joel Ribis[1], Patricia Donnadieu[2,3], Camille Flament[4], Marie-Loyer Prost[4], and Frédéric Leprêtre[4]

[1.] DEN-Service de Recherches Métallurgiques Appliquées, CEA, Université Paris-Saclay, Gif-sur-Yvette, France.
[2.] Université Grenoble Alpes, SIMAP, Grenoble, France.
[3.] CNRS, SIMAP, Grenoble, France.
[4.] DEN-Service de Recherches de Métallurgie Physique, CEA, Université Paris-Saclay, Gif-sur-Yvette.

There are a number of operational environments where the performance of materials is likely to be affected significantly by fast-particle irradiation. These include amongst others: fission and fusion reactors, nuclear waste storage containers, particle accelerators, and spacecraft [1]. Thus, understanding the basic processes involved when materials are exposed to energetic particle irradiation is a key point in the choice of materials for use in such environments. During irradiation when energetic particles interact with the material, the target atoms are displaced from their original position in the crystal resulting in the production of a high density of defects, namely vacancies and interstitial atoms. The condensation of these supersaturated vacancies into cluster defects, and further growth by absorption of defects of the same type results in the formation of cavities. The term cavities refers to voids as well as bubbles. Cavities can be imaged using Fresnel contrast [2] which arises from the phase shift generated by the variation of the mean inner potential of the matrix owing to atom deficiency caused by cavities [2]. The effect depends sensitively on the amplitude value of under- or overfocus of the objective lens. In an under-focused image, cavities appear as dark Fresnel fringes surrounding a bright dot, while in an over-focused image, cavities appear as bright fringes surrounding a dark dot. In order to go further in this phase contrast approach, the phase shift between electrons which traverse the cavity and those which pass through adjacent perfect crystal may be retrieved by using in-line electron holography.

In-line electron holography is named after the fact that no external reference wave exists, i.e. the object wave itself is its own reference wave [3]. This allows for a simpler experimental setup rather than using a dedicated holography device. Further, in-line holograms may be acquired anywhere within the specimen. In-line holography consists in the reconstruction of the complex electron wave function from a Fresnel image series, to determine local variations in the mean inner potential of the scattering specimen [4]. Under the assumption that there is no multiple scattering, no diffraction and absorption contrast and for small shift (< 1rd), the so-called weak phase object approximation allows to write the intensity of an image taken at a defocus Δz in the reciprocal space as follows [5]:

$$\hat{I}(q,\Delta z)=I_0\left(1-2\hat{\Phi}(q)sin\left(\pi\lambda\Delta z q^2+C_s\lambda^3 q^4\right)\right) \quad (1)$$

where $\hat{I}(q,\Delta z)$ is the Fourier transform of the image intensity, q is the spatial frequency, Δz is the defocus, I_0 is given by the average intensity of the image at zero defocus, $\hat{\Phi}(q)$ is the phase shift Fourier transform, λ is the electron wavelength and C_s is the spherical aberration constant.
Under small angle approximation the phase shift can be retrieved from a series of three images taken at defocus values $+\Delta z$, 0, $-\Delta z$ using the following equation:

$$\hat{\Phi}(q)=\frac{1}{I_0}\frac{1}{4\pi\lambda q^2}\frac{\Delta\hat{I}(q)}{\Delta z} \quad (2)$$

Where $\Delta\hat{I}(q)$ is the Fourier transform of the difference between the images taken at defocus $+\Delta z$ and $-\Delta z$. This relation is appropriate for system characterized by spatial variations described by a wave vector $q < (2\pi\lambda\Delta z)^{-1/2}$. Consequently, the spatial resolution is limited to the value $d > (2\pi\lambda\Delta z)^{1/2}$[6, 7]. Under

kinematical conditions, the phase shift could be estimated from the mean inner potential of the sample and written as [5] :

$$\widehat{\Phi}(q) = C_E V_0 t \quad (3)$$

Where V_0 is the mean inner potential, t the sample thickness, C_E the interaction constant depending on the accelerating voltage. As cavities correspond to the absence of atoms, they are expected to locally decrease the mean inner potential and therefore generate a negative phase shift on the traversing electron wave. Figure 1 (a) shows a TEM image of an ion irradiated 6061-T6 aluminium alloy while Figure 1 (b) shows the corresponding phase map retrieved from focal series using in-line holography method as described above. The irradiation conditions are presented elsewhere [7]. The blue-green colored domains correspond to a zero radian phase shift while the blue color domains correspond to a positive phase shift (as illustrated by the AlCrFeMnSi precipitate in the middle in the Figure 1b) and the red colored domains correspond to a negative phase shift. Thus, these last domains correspond to a mean inner potential decrease and can be interpreted as cavities. Further, the phase images are very convenient for quantitative analyses. For instance the phase map can be easily binarized: considering the negative phase shift as threshold (figure 1 (c)) make all cavities appear white. The density has been then estimated to be about 9.9×10^{22} m^{-3} (assuming a 100 nm thickness).

In conclusion, a simplified version of in-line holography has been successfully applied for imaging cavities in ion-irradiated aluminium alloy. The fluctuation of the matrix inner potential owing to the presence of voids, make the retrieval of phase shift a very convenient tool for imaging and counting cavities in irradiated alloys [8].

References:

[1] ML Jenkins and MA Kirk in "Characterization of Radiation Damage by Transmission Electron Microscopy", ed. B. Cantor, M.J. Coringe, (IOP, Bristol and Philadelphia) p. 1.
[2] ML Jenkins, J. Nucl. Mater. **216** (1994), p. 124.
[3] CT Koch, Ultramicroscopy **108** (2008), p. 141.
[4] S Bhattacharya, CT Koch and M Rühle, Ultramicroscopy **106** (2006), p. 525.
[5] L Reimer, Transmission Electron Microscopy, 2nd ed., (Springer Verlag, Berlin).
[6] P Donnadieu et al., Appl. Phys. Lett. **94** (2009), p. 263116.
[7] J Ribis et al., Phil. Mag. **96** (2016), p. 2504.
[8] Irradiations at SRMP-JANNuS Saclay were performed thanks to the funding of the EMIR network.

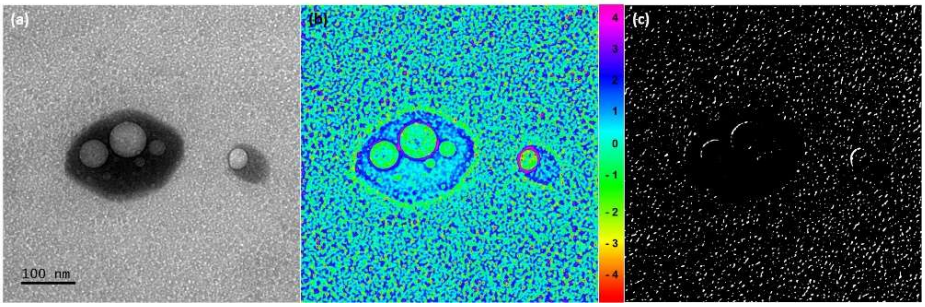

Figure 1. 6061-T6 aluminium alloy after ion irradiation (150 dpa): (a) TEM image at defocus 0 nm, (b) Phase map retrieved from a focal series (+ 100 nm, - 100 nm) using the in-line holography method (colored scale in radian), (c) Binary image processed with a negative phase shift threshold where the white features are the cavities

https://doi.org/10.1017/S1431927619008511 Published online by Cambridge University Press